The mechano-sensitive ion channel Piezo mediates Rho activation and actin stress fibre formation in *Drosophila* nephrocytes

Sybille Koehler. PhD [1,2], Ilka Edenhofer [2], Maja Lindenmeyer, PhD [2], Thorsten Wiech, MD [3], Tobias B. Huber, MD [2] and Barry Denholm, PhD [1]

[1] Biomedical Sciences, University of Edinburgh, Edinburgh, Scotland, UK; [2] III. Department of Medicine, University Medical Center Hamburg-Eppendorf, Hamburg, Germany; [3] Nephropathology Section, Institute of Pathology, University Medical Center Hamburg-Eppendorf, Hamburg, Germany

Corresponding author:

Sybille Koehler

Hugh Robson Building
George Square
EH89XD Edinburgh
Scotland, UK

Current address:
Campus Forschung N27
Martinistraße 52
UKE Hamburg
20246 Hamburg
Germany

Sy.koehler@uke.de

Word count: 4165

Keywords: Podocyte, Mechanosensation, glomerular disease

Running title: Piezo mediates Rho activation in nephrocytes

Abstract

Due to their exquisite position on glomerular capillaries, podocytes are continuously counteracting biomechanical filtration forces. Most therapeutic interventions known to generally slow or prevent the progression of chronic kidney disease appear to lower the biochemical forces on podocytes, highlighting the critical need to better understand podocyte mechano-signalling pathways.

Here we investigated the hypothesis that the mechanotransducer Piezo is involved in a mechanotransduction pathway in *Drosophila* nephrocytes, the podocyte homologue

in the fly. We find Piezo is expressed in nephrocytes and podocytes and localizes to the slit/nephrocyte diaphragm. Piezo activation leads to a significant increase in intracellular Ca^{++} upon exposure to shear stress and an activation of Rho1 in nephrocytes. Loss of function analysis in Piezo knockout nephrocytes revealed only minor defects in nephrocyte filtration function. In contrast, we show that elevated Piezo levels resulted in constitutive Ca^{++} oscillations even in the absence of shear stress, increased active Rho1 and accumulation of actin stress fibers, culminating in a severe nephrocyte filtration phenotype, suggesting that pathway hyperactivity is detrimental. Blocking Piezo activity using the tarantula toxin GsMTx4 reversed levels of activated Rho1 into the normal range. Thus, Piezo-mediated mechano-signalling acts as surveillance mechanism by which nephrocytes sense and adapt to changes in mechanical force.

Introduction

Kidney podocytes are highly specialized epithelial cells, which together with the fenestrated endothelium and the glomerular basement membrane, constitute the three-layered, size and charge selective filter of the glomerular filtration barrier [1]. Podocytes have a unique morphology, forming primary and secondary foot processes which completely enwrap the capillaries. Injury of podocytes causes severe morphological change, detachment from the basement membrane and finally loss of podocytes into primary urine. Until today several genes are described to be important for podocyte biology, among them are NPHS1, NPHS2, TRPC6 and Actinin-4 [2–6]. Loss of podocytes has pathological consequences as these cells are post-mitotic and cannot be replenished. The blank capillaries are not sealed anymore resulting in massive loss of protein from blood into urine, so called proteinuria. Podocyte injury can

occur because of genetic deficiencies [2–6], toxin-mediated triggers [7] and changes in the physical environment within the glomerulus [8–11].

Podocytes are under constant mechanical force and regularly face changes in in these forces, as they are responsible for the filtration of ~180 litres of primary urine each day. The main forces arising from this are hydrostatic pressure (50 kPa) and fluid shear stress at the filtration slits (8 Pa) [12]. These forces increase during diseases such as diabetes and hypertension and result in podocyte loss [10]. Progressive loss of podocytes leads to a vicious cycle as biomechanical forces experienced by those cells remaining increase further. It is known remaining podocytes respond by growing in size to re-cover the blank capillary to overcome the challenge originating from loss of neighbouring cells; this is considered to be an adaptive and protective mechanism [13–15]. In order for this to happen, podocytes must exhibit mechnotransductive mechanisms to recognize these changes in the physical environment and initiate adaptive and protective responses, likely candidates are TRPC6, YAP, Talin and Filamins and Piezo [5,8,9,16–19].

Piezo is a mechanosensitive ion channel that is involved in mechanotransduction in many development and physiological contexts. Piezo channels (Piezo1 and Piezo2) open in response to mechanical force and allow the influx of positively charged ions such as Ca^{++} and Na^{+} [20,21]. The two proteins have different functional roles as Piezo1 was reported to be essential for sensing blood flow-associated shear stress and blood vessel development [22–24], while Piezo2 responds to touch and proprioception [25]. Piezo1 is expressed in podocytes however it is unknown if it is involved in a mechanotransduction pathway in these cells, and if so how it might function [19].

To address these questions, we used the *Drosophila* nephrocyte model and investigated the effect of Piezo depletion and activation on nephrocyte morphology

and function. Nephrocytes form foot processes, which are spanned by the nephrocyte diaphragm, a highly-specialized cell-cell contact, that is highly similar to the mammalian filtration barrier in the glomeruli [26,27]. They function as filtration units in the fly and filter toxins and waste products from the haemolymph. Our data show that nephrocytes respond to shear stress with an increase of intracellular Ca^{++} levels. Moreover, we could show that the mechanotransducer Piezo is expressed in nephrocytes and localizes to the nephrocyte diaphragm. Piezo loss of function results in a mild phenotype. In contrast hyperactivation of Piezo caused severe filtration defects, significant activation of Rho1 and accumulation of actin stress fibers. Thus, our data confirms, that Piezo is involved in a mechanotransduction pathway in nephrocytes and its hyperactivity is detrimental for nephrocyte function.

Material and Methods

Table 1: List of antibodies

Name	**Company/ Provider**	**Catalog nr. / Reference**	**Host Species**	**Dilution IF**
Duf	M. Ruiz-Gomez	[26]	Rabbit	1:100
Pyd	Developmental Studies Hybridoma Bank	PYD2	Mouse	1:25
Piezo1	Novus Biologicals	NBP1-78537-0.025ml	Rabbit	1:25
Piezo2	Novus Biologicals	NBP1-78624SS	Rabbit	1:50

Synaptopodin	Synaptic Systems	163 004	Guinea Pig	1:200

Table 2: List of fly strains

Fly strain	Origin	Purpose	Chromosome
Piezo MI{MIC}	BDSC ID: 60209	Endogenous GFP-tag	2. Chr.
Piezo^{ko}	BDSC ID: 58770	Knockout	2. Chr.
UAS-*piezo*-GFP	BDSC ID: 58773	Overexpression	3. Chr.
UAS-*piezo*-RNAi	VDRC ID: 101915	Knockdown	2. Chr.
UAS-*sns*-RNAi	VDRC ID: 109442	Knockdown	2. Chr.
UAS-*duf*-RNAi	VDRC ID: 27227	Knockdown	2. Chr.
sns-Gal4; UAS-*dicer*2	[8]	Nephrocyte-specific driver	2. + 3. Chr.
UAS-Rok-RBD-GFP	BDSC ID: 52290	Rho1 sensor	3. Chr.
sqh-Pak-RBD-GFP	BDSC ID: 56550	Rac/Cdc42 sensor	3. Chr.
UAS-LifeAct-RFP	BDSC ID: 58362	Overexpression	3. Chr.
UAS-GCamP6medium	BDSC ID: 42750	Overexpression	3. Chr.
Oregon R		wildtype	
W^{1118}		wildtype	

Fly husbandry and generation

For experiments all flies were kept at 25°C. The nephrocyte-specific knockdown or overexpression was achieved by mating UAS fly strains with the *sns*-Gal4 strain.

YODA and GsMTx4 treatment

To active Piezo acutely nephrocyte were incubated with the specific activator compound YODA (10nm in DMSO; control: DMSO) (Sigma, now Merck). To inhibit mechano-sensitive channels in an unspecific way nephrocytes were incubated with

tarantula toxin/GsMTx4 (5μM in H_2O; control: HL3 buffer) (Alomone labs, Jerusalem, Israel, Cat. nr: STG-100). For all experiments nephrocytes were isolated as described below in haemolymph-like buffer (HL3.1; 70 mM NaCl, 5 mM KCl, 1.5 mM $CaCl_2$, 4 mM $MgCl_2$, 10 mM $NaHCO_3$, 115 mM Sucrose and 5 mM Hepes). Cells were then incubated for 5 mins followed by a washing step in HL3 for one min. Nephrocytes were fixed for 20 mins with 4 % formaldehyde before mounting.

Immunofluorescences of *Drosophila* tissue

Garland nephrocytes were isolated from 3rd instar larvae in HL3 buffer. After isolation cells were fixed in 4 % formaldehyde for 20 mins, followed by three washing steps with washing buffer (Phosphate buffer saline, 0.5% bovine serum albumin, 0.03% Triton-X) for 20 mins. Primary antibody incubation was done overnight at 4°C. On day 2, the cells were washed three times for 20 mins, incubated with 5 % normal horse serum for 30 min and 1 h with the respective secondary antibody. Afterwards followed three washing steps for 20 mins and mounting with mounting medium (2.5% propyl gallate and 85% glycerol). Imaging was done using either a Zeiss LSM 8 confocal combined with an Airyscan for higher resolution or a Leica SP8 confocal. Images were further processed using ImageJ (version 1.53c).

Immunofluorescence of mammalian tissue

Paraffin-embedded tissue from wildtype mice and patient derived kidney tissue (obtained from Nephropathology Section, Institute of Pathology, University Medical Center Hamburg-Eppendorf, Hamburg, Germany) was used for immunofluorescence stainings. Tissue was de-paraffinized by passing through a descending alcohol row. After washing for three times (5 mins) with H_2O followed by three washing steps with Dako wash buffer (Agilent Technologies, Santa Clara, USA), antigen retrieval was

done in a steamer using pH9 antigen retrieval from Dako. Primary antibodies (listed in Table 1) were diluted in Dako antibody diluent and incubated overnight at 4°C. The next day sections were washed for three times (5 mins) with Dako wash buffer, followed by secondary antibody incubation with DAPI for one hour at room temperature. Prior to mounting with Prolong Gold, samples were again washed for three times. Imaging of samples was done at a Zeiss LSM 900 confocal. Images were further processed using ImageJ (version 1.53c).

FITC-Albumin uptake assay

FITC-Albumin uptake assays were performed as previously published [8,28]. Garland nephrocytes were isolated from 3rd instar larvae and incubated with FITC-Albumin (0,2 mg/ml; Sigma-Aldrich, St. Louis, USA) for 1 min, followed by 20 mins fixation with 4 % Formaldehyde. Imaging was done with a Zeiss LSM 5 confocal or Leica SP8 confocal microscope and images were further processed and analyzed using ImageJ (version 1.53c). For comparative analysis, the exposure time of experiments was kept identical. The mean intensity of FITC-Albumin was measured and normalized to control cells. Images were also used to quantify nephrocyte size by measuring the area of each cell.

$AgNO_3$ toxin assay

Flies of the appropriate genotype were allowed to lay eggs for 24 hrs at 25°C on juice plates with normal yeast. Afterwards, plates with eggs were kept at 18°C for 24 hrs. 1st instar larvae were then transferred to juice plates supplemented with yeast paste containing $AgNO_3$ (2 g yeast in 3.5 ml 0.003% $AgNO_3$). Plates were kept at 25°C for 4 days to let larvae develop and pupate. 5 days after egg laying pupae were counted daily for 4 consecutive days. The number of pupae was normalized to the number of 1st instar larvae transferred to the plates.

Quantification of GTPase activity levels

To quantify activity levels of Rho1 and Rac/Cdc42 in garland nephrocytes. UAS-Rok-RBD-GFP and UAS-Pak-RBD-GFP flies were combined with the nephrocyte-specific driver *sns*-Gal4. For final matings, these flies were either combined with UAS-*piezo*-RNAi or UAS-*piezo*-GFP flies. Garland nephrocytes from 3rd instar larvae were isolated and fixed for 20 mins with 4 % Formaldehyde followed by mounting with mounting medium. Images were obtained using a Leica SP8 confocal and further image processing was done using ImageJ (version 1.53c). The mean GFP intensity was measured and normalized to cell size prior to normalization to control cells. For comparative analysis, laser intensity and settings were kept equal.

Visualization of the actin filaments

For actin cytoskeleton visualization, the nephrocyte-specific driver *sns*-Gal4, UAS-LifeAct-RFP and UAS-Piezo-GFP flies were combined. Garland nephrocytes were isolated from 3rd instar larvae and fixed for 20 mins with 4 % Formaldehyde, prior to mounting with mounting medium. Images were obtained using a Leica SP8 confocal. Further image processing was done using ImageJ (version 1.53c). For quantification mean intensities of RFP were measured and normalized to cell size. For comparative analysis, laser intensity and settings were kept equal.

Ca^{++} imaging of pericardial nephrocytes

For Ca^{++} imaging purposes UAS-GCamP6 flies were combined with the nephrocyte-driver *sns*-Gal4 and mated with UAS-*piezo*-RNAi or UAS-*piezo*-GFP to obtain experimental animals. Flies were kept at 25°C until the experimental flies were 1-5 days old. For *ex vivo* Ca^{++}-imaging only male flies were used. Pericardial nephrocytes

were isolated, but still attached to the heart tube and the cuticle. The tissue was kept in HL3.1 buffer. For imaging a Zeiss Axio Examiner microscope with a x40 dipping objective, fitted with GFP filters and LED light source (Carl Zeiss Ltd.) and connected to a Prime 95B sCMOS camera (Photometrics) running from Micro-Manager 1.4 software was used. Images were acquired every second for 150 secs and after 60 secs a wave was induced by pipetting HL3.1 buffer into the dish with the tissue. For quantification of the GCamP6 signal a previously published FIJI macro was used [29]. For comparative analysis, the mean of the first 10 measurements of every cell was used for quantification ($F/_{F1-10}$). To quantify the signal amplitude parameters (height and width), values after normalization were used. To determine baseline values raw data was used.

Microarray analysis.

Human renal biopsy specimen and gene expression profiles were obtained within the framework of the European Renal cDNA Bank - Kröner-Fresenius Biopsy Bank [30]. Diagnostic biopsies were obtained from patients after informed consent and with approval of the local ethics committees. Sample collection, RNA isolation and preparation, and microarray analysis were performed as described previously [31]. Glomerular samples from patient with different renal diseases were analyzed for mRNA expression levels (GSE32591, GSE35489, GSE37463, GSE47185, GSE 99340). The analysis included gene expression profiles from patients with DN (n=14 glomeruli), hypertensive nephropathy (HT; n=15), MCD (n=14), IgA nephropathy (IgA; n=27), FSGS (n=23), membranous nephropathy (MGN; n=21), lupus nephritis (SLE; n=32), ANCA-associated glomerulonephritis (RPGN; n=23), and controls (LDs; n=41). CEL file normalization was performed with the robust multichip average method using RMAExpress (Version 1.0.5) and the human Entrez-Gene custom CDF annotation

from Brain Array version 25 (http://brainarray.mbni.med.umich.edu/Brainarray/default.asp). The log-transformed dataset was corrected for batch effect using ComBat from the GenePattern pipeline (http://www.broadinstitute.org/cancer/software/genepattern/). To identify DEGs, the Significance Analysis of Microarrays (SAM) method [32] was applied using the SAM function in Multiple Experiment Viewer (TiGR MeV, Version 4.9). A q-value below 5% was considered to indicate statistical significance.

Statistical analysis

To determine statistical significance Graph Pad Prism software version 8 for Mac (GraphPad Software, San Diego, CA) was used. All results are expressed as means ± SEM. Comparison of two groups was done using a student's t-test. A *P-value* < 0.05 was considered statistically significant. Comparison of more than two groups with one independent variable was done using one-way ANOVA followed by Tukey's multiple comparisons test. A *P-value* < 0.05 was considered statistically significant.

Ethics

The human renal biopsy studies have been performed in accordance with the law of Hamburg hospitals (HmbKHG, §12).

Results

***Drosophila* nephrocytes respond to shear stress by Ca^{++} influx**

Podocytes rely on Ca^{++} as a second messenger, but increased and prolonged Ca^{++} influx results in podocyte injury and loss, as seen for gain-of-function mutations of the cation channel TRPC6 [5,33]. Here, we wanted to test the hypothesis that nephrocytes also rely on Ca^{++} as second messenger and whether they respond to

shear stress by opening of mechano-sensitive channels, which subsequently results in Ca^{++} influx.

We isolated pericardial nephrocytes from adult flies, which express the Ca^{++} sensor GCAmP6m. We induced shear stress by washing a stream of buffer over the cells. This induction of shear stress resulted in an immediate increase of the Ca^{++} signal intensity (GCAmP6m) in nephrocytes **(Figure 1A third image and B left panel)**. The maximum amplitude in control cells is reached after 2 secs and returns to baseline levels after 5 secs. This data confirms that nephrocytes respond to shear stress with an immediate single Ca^{++} transient. This is consistent with the opening of surface mechanosenstive ion channels resulting in Ca^{++} influx.

We next asked, if this mechanism is disturbed in injured nephrocytes. To induce injury, we depleted nephrocytes for Duf (dNEPH) or Sns (dNephrin), which results in a severe morphological and functional phenotype in nephrocytes [26,27]. The Ca^{++} transient amplitude (signal intensity) and signal duration after shear stress was significantly reduced in Duf- or Sns-depleted nephrocytes **(Figure 1A,B,C,D)**. In addition, GCamP6 baseline intensity was significantly reduced **(Figure 1E)**, suggesting a major perturbation of Ca^{++} signalling upon nephrocyte injury. We also measured the kinetics of the Ca^{++} transient in the injured nephrocytes and observed similar kinetics in the Sns knockdown cells when compared to controls (maximum amplitude in Sns knockdown cells is reached after 2 secs and returns to baseline levels after 5 secs). Depletion of Duf however resulted in a slower increase of intracellular Ca^{++} levels, as the maximum amplitude was reached after 3 secs and returns to baseline after 4 secs. Our data confirms that nephrocytes respond to shear stress by Ca^{++} influx, which is consistent with the hypothesis that mechanotransduction is an inherent property of nephrocytes.

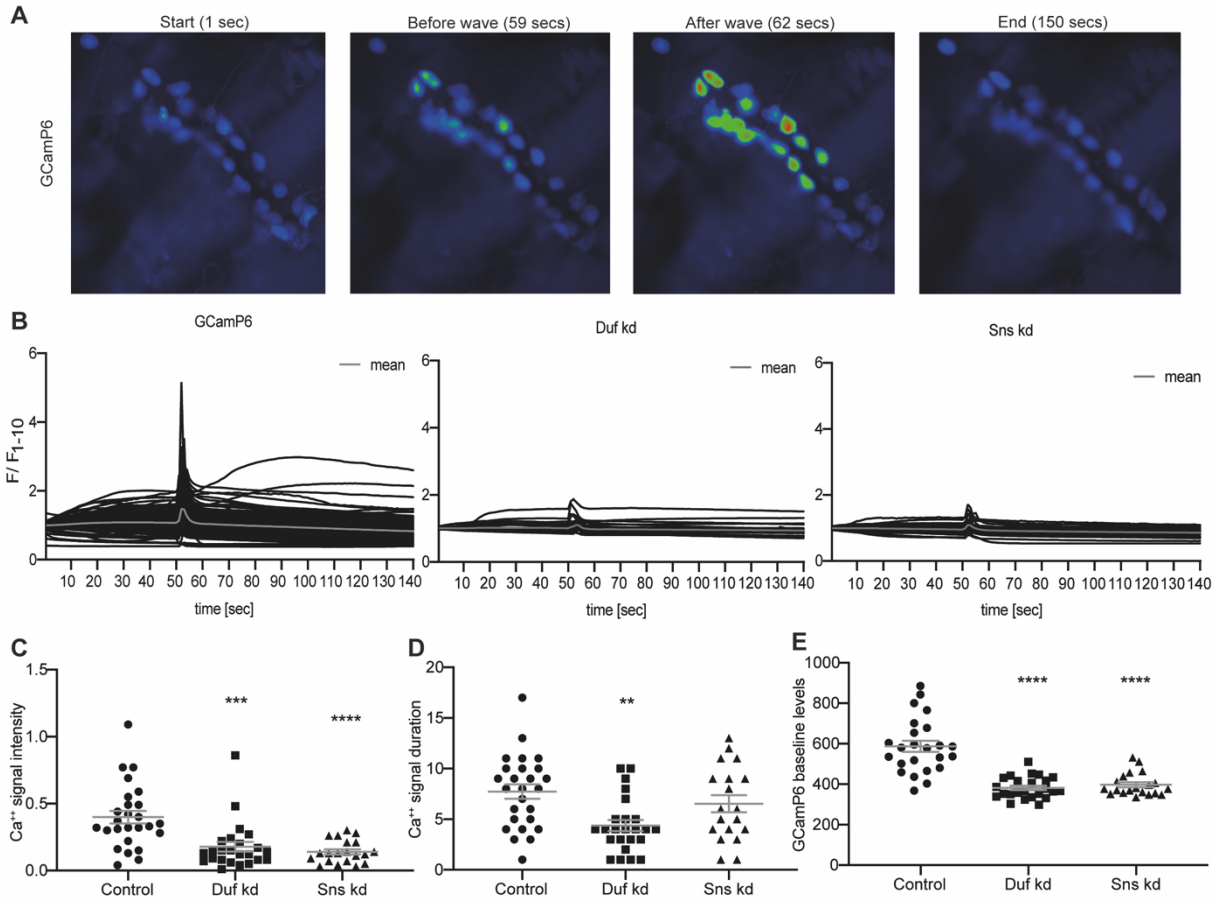

Figure 1: Nephrocytes respond to shear stress by an increased Ca^{++} influx, while loss of the nephrocyte diaphragm proteins Sns and Duf results in disturbances of Ca^{++} signalling. A,B Ca^{++} signalling events were recorded for 150 secs. After 60 secs shear stress was induced by adding buffer and an immediate Ca^{++} signal was recorded, which is depicted by the peak in the graph. This peak was significantly smaller in Duf and Sns knockdown nephrocytes, when compared to GCAmP6 controls. Control: w; *sns*-Gal4/+;UAS-*GCAmP6m*/+; Duf kd: w; *sns*-Gal4/ UAS-*duf*-RNAi;UAS-*GCAmP6m*/+; Sns kd: w; *sns*-Gal4/ UAS-*sns*-RNAi;UAS-*GCAmP6m*/+. **C** Peak Ca^{++} signal intensity was significantly reduced in the knockdown cells. 1way ANOVA with Tukey's multiple comparison test: ***: $p < 0.001$; ****: $p < 0.0001$. **D** Peak duration was also significantly reduced after depleting Sns and Duf. 1way ANOVA with Tukey's multiple comparison test: **: $p < 0.01$. **E** Baseline GCAmP6 intensity was also measured and showed a significantly reduced intensity in the knockdown cells, when compared to controls. 1way ANOVA with Tukey's multiple comparison test: ****: $p < 0.0001$.

Piezo is expressed in nephrocytes and localizes to the nephrocyte diaphragm

The mechanotransducer Piezo opens upon mechanical force, leading to the influx of Ca^{++} (and other cations) and is therefore a candidate for this mechanism. It was reported that Piezo1 is expressed in podocytes, but the exact localisation pattern is not known [19]. Until today Piezo expression has not been studied in nephrocytes. Hence, here we examined Piezo expression in nephrocytes and could show co-localisation with the nephrocyte diaphragm proteins Duf, the NEPH homolog in the fly,

and Pyd (dZO1), suggesting Piezo is a component of the nephrocyte diaphragm multi protein complex **(Figure 2A)**. A previous study revealed Piezo1 expression in mouse glomeruli [19], further supporting our hypothesis that Piezo is expressed in podocytes and nephrocytes and is involved in mechanotransduction pathways not only in *Drosophila*, but also mammals. High resolution microscopy of Duf and Pyd at the surface of the nephrocyte revealed a fingerprint-like pattern highlighting the nephrocyte junction. At this resolution, Piezo showed strong co-localisation with Duf, while Pyd and Piezo present with a distinct localisation pattern. These data reinforce the hypothesis that Piezo is a component of the nephrocyte diaphragm. It remains to be tested whether there is direct interaction between any of these proteins. In addition, we examined expression of Piezo 1 and Piezo 2 in mammalian podocytes, by co-visualization with the podocyte marker Synaptopodin **(Figure 2C,D)**. Both, Piezo 1 and Piezo 2, show expression in podocytes. This finding can be further confirmed by analysing published proteomics data from isolated primary mouse podocytes, in which both proteins were found to be expressed in the podocyte population [34].

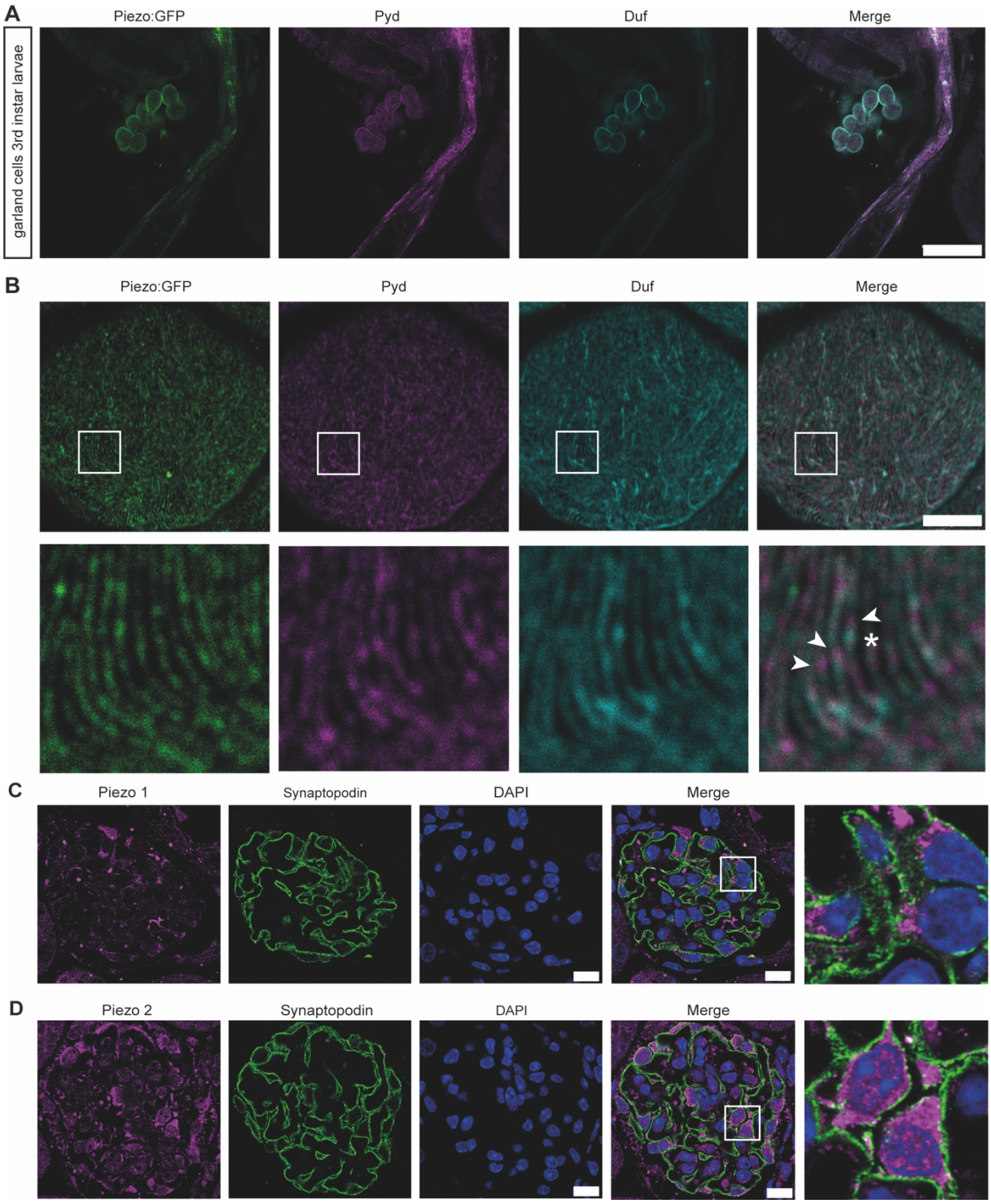

Figure 2: Piezo is expressed in nephrocytes and localizes to the nephrocyte diaphragm. A Immunofluorescence staining with a Duf (dNEPH) and Pyd (dZO1) antibody revealed expression and localisation of Piezo (Piezo:GFP; Mi{MIC} line) at the nephrocyte diaphragm in garland nephrocytes from 3rd instar larvae . Scale bar = 50 μm. **B** High resolution microscopy showed co-localisation of Piezo and Duf, while Pyd and Piezo presented with a distinct localisation pattern. Arrow heads: Pyd, Star: Piezo and Duf. Scale bar = 5 μm. **C,D** Piezo1 and Piezo2 are expressed in mammalian podocytes, which are visualized using the podocyte marker Synaptopodin. Scale bar = 10 μm.

Pharmacological activation of Piezo with YODA results in increased Rho1-GTP levels

To address, whether Piezo exhibits a functional role in nephrocytes, we investigated the effects of pharmacological activation of Piezo. To do so, we used YODA, which is a chemical compound which specifically facilitates Piezo opening at lower magnitude of force [35,36]. As Piezo is a Ca^{++} permeable cation channel and known to be important for Ca^{++} influx, we investigated the effect of YODA by measuring Ca^{++} levels in nephrocytes. Piezo channels are sensitive to mechanical stimuli and stretch, hence here we induce shear stress and measured the immediate Ca^{++} signal intensity (GCAmP6 peak), duration and the baseline GCamP6 levels.

5-minute incubation of pericardial cells with YODA resulted in a significant increase of both, the amplitude (signal intensity) and signal duration, after induction of shear stress and when compared to DMSO incubated cells (controls) **(Figure 3A)**. Interestingly, baseline levels of GCamP6 intensity (before applying shear stress) were significantly lower in cells incubated with YODA for 5 mins, suggesting that potential compensatory pathways of Ca^{++} efflux might be activated. The increased Ca^{++} signal intensity and duration upon incubation with YODA provides additional support for a Piezo-dependent mechanotransduction mechanism in nephrocytes. Moreover, it also supports the hypothesis that Piezo is involved in a mechanotransduction pathway in nephrocytes which is mediated via Ca^{++} influx. We investigated whether the YODA mediated Piezo sensitization had short-term phenotypic consequences on nephrocyte morphology and filtration function. Analysis after a 5 minute incubation with YODA did not cause any changes in morphology of the filter slit, nor filtration function as assessed with the FITC Albumin uptake assay, when compared to DMSO incubated controls **(Figure 3B,C)**.

Ca^{++} is a second messenger in cells and can act by modulating GTPase activation. It is known that over-activation of the GTPases RhoA and Rac1 results in podocyte injury in mice [37–39]. Hence, we measured the activity levels of the GTPases Rho1 and Rac/Cdc42 in nephrocytes treated with DMSO or YODA to determine if these were downstream components of the pathway. We used Rok-RBD (a Rho1 sensor) and Pak-RBD (a sensor that reports on activity of Rac and Cdc42) to visualize active Rho1 and Rac/Cdc42 activity in nephrocytes. Interestingly, analysis revealed a significant increase of active Rho1 levels while Rac/Cdc42 activation was significantly inhibited after YODA incubation **(Figure 3D,E)**.

Both, Ca^{++} and GTPases, have an impact of actin stress fibre formation. Therefore, we visualized the actin cytoskeleton by using flies expressing RFP-LifeAct in nephrocytes. Previous work revealed the presence of cortical stress fibres and actin clusters in *Drosophila* nephrocytes [40]. Although GTPase activation levels were altered by YODA treatment, no differences of actin stress fibre or cluster formation could be observed in comparison to control cells **(Figure 3F)**. This could either be explained by the short time between YODA incubation and imaging the cells or a missing effect on the actin cytoskeleton by acute activation of the channel. Taken together, the pharmacological activation of Piezo by YODA demonstrates a functional role of the channel in nephrocytes and delineates a mechanotransduction pathway, involving Ca^{++} signalling and GTPases.

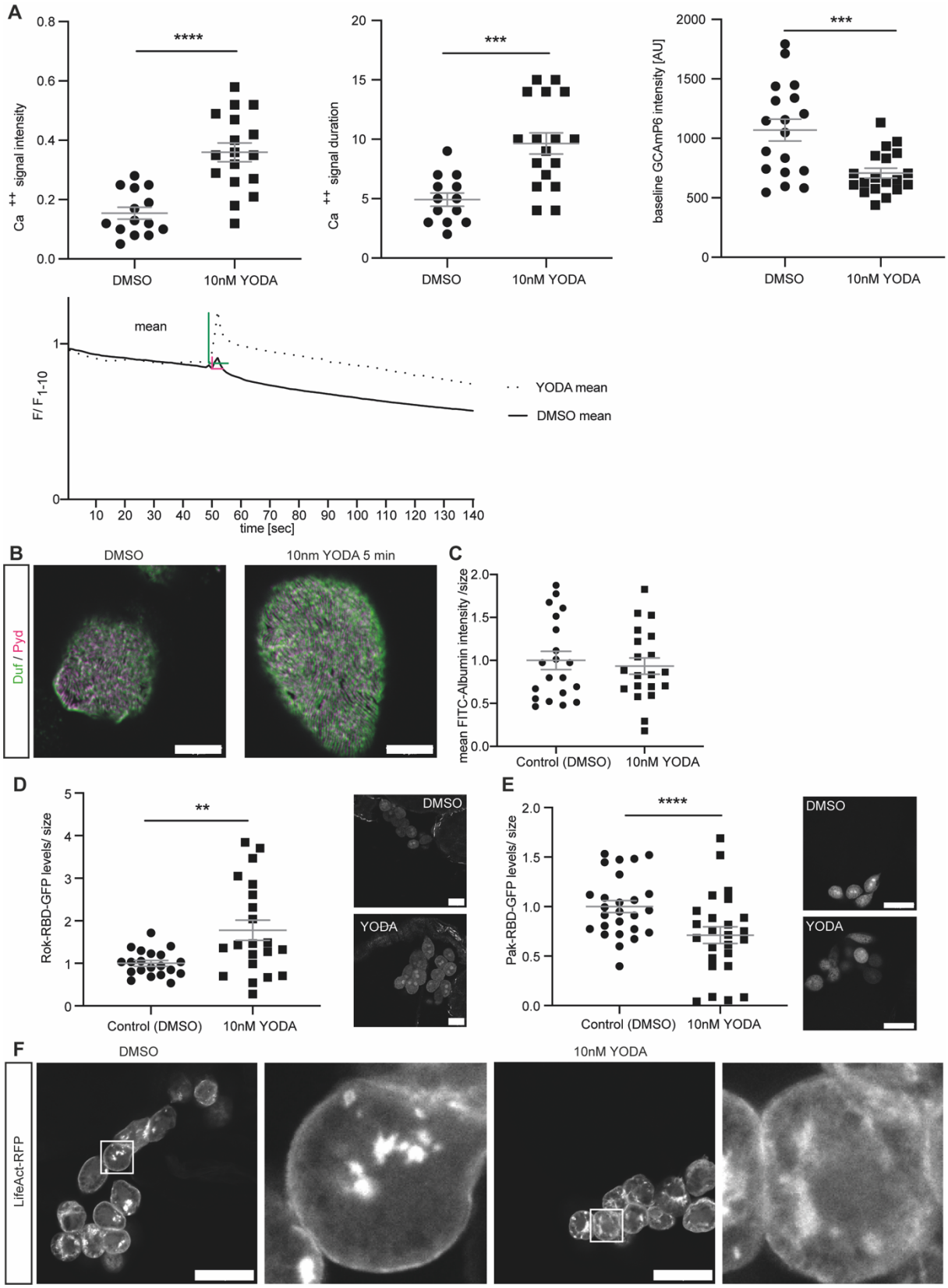

Figure 3: Pharmacological activation of Piezo causes Rho1 activation. A Ca^{++} signalling events were recorded after Piezo activation with YODA and after inducing shear stress after 60 sec. The immediate Ca^{++} wave observed after the induction of shear stress was significantly higher (peak intensity/amplitude; green and magenta line) and longer (peak duration; green and magenta line) in pericardial cells incubated with YODA when compared to controls (DMSO). Baseline Ca^{++} (GCAmP6m) levels were significantly reduced after 5 min incubation with YODA. Student's t-test: ***: $p < 0.001$, ****:

$p < 0.0001$. Visualisation of mean values of the DMSO and YODA treated nephrocytes show the differences in the amplitude after shear stress induction. The green and magenta lines depict the differences in amplitude height and width. w; *sns*-Gal4/+;UAS-*dicer2*/UAS-*GCAmP6m*. **B** 5 min incubation with YODA did not reveal any morphological changes as depicted by immunofluorescence staining with a Duf and Pyd antibody. Scale bar = 5 μm. **C** The FITC-Albumin uptake assay did not reveal any differences between controls (DMSO) and YODA treated cells. FITC-Albumin intensity was normalized to nephrocyte size. **D** Quantification of active Rho1 levels (Rok-RBD-GFP) revealed a significant increase of Rho1-GTP levels after YODA incubation (scale bar = 25 μm), while **E** Rac/Cdc42-GTP levels were significantly decreased as depicted with Pak-RBD-GFP flies (scale bar = 50 μm). Student's t-test: *: $p < 0.05$; **: $p < 0.01$. w; *sns*-Gal4/+;UAS-*dicer2*/UAS-*rok-RBD*-GFP (**D**); w; *sns*-Gal4/+;UAS-*dicer2*/sqh-*pak-RBD*-GFP (**E**). **F** Visualisation of the actin cytoskeleton (LifeAct-RFP) did not reveal any changes upon YODA treatment. Scale bar = 50 μm. w; *sns*-Gal4/+;UAS-*dicer2*/UAS-LifeACT-RFP.

Loss of Piezo resulted in only a mild filtration defect

After the expression of Piezo in nephrocytes was confirmed, we wanted to know if Piezo is important for nephrocyte morphology and function. To address this question, we examined nephrocyte diaphragm morphology and filtration function in animals completely lacking Piezo ($Piezo^{KO}$). Loss of Piezo did not result in any changes of the slit diaphragm integrity as assessed by immunofluorescence **(Figure 4A)**. FITC Albumin uptake assays revealed a significant increase of uptake after depletion of Piezo (whole body knockout and nephrocyte-specific depletion) **(Figure 4B,C)**. However, the FITC Albumin assay cannot distinguish between uptake, filtration and endocytosis. To assess the effect of Piezo depletion on filtration function in more detail, we performed the $AgNO_3$ toxin assay. During larval development nephrocytes are important to clear the haemolymph from toxins and waste products to ensure normal development. By feeding larvae $AgNO_3$, the toxin will accumulate in the haemolypmh and needs to be cleared by nephrocytes to prevent a developmental delay (pupation delay). Impaired filtration function will result in less clearance efficiency and therefore cause a developmental delay of larvae, which can be used as an indirect way to assess filtration function. As the $Piezo^{KO}$ lesion is in a w^{1118} background ($Piezo^{KO}$ was backcrossed into w^{1118} for six generations prior to experiments), we used this strain as a control for the $Piezo^{KO}$. Interestingly, the w^{1118} strain presented with a delayed

pupation, which was similar to the Piezo^{KO}, suggesting that the filtration defect is not caused by depletion of Piezo, but rather due to the genetic background **(Figure 4D)**. To further confirm, that loss of Piezo does not influence filtration function and therefore pupation, we also used a Piezo-RNAi fly strain to deplete Piezo only in nephrocytes and could show, that a knockdown of Piezo also did not reveal any differences in pupation when compared to control flies **(Figure 4E)**.

Here, we showed an impact of pharmacological activation of Piezo on Ca^{++} signalling and GTPase activation **(Figure 3)** and wanted to know whether depletion of Piezo results in defects in Ca^{++} signalling and altered GTPase activity levels as well. To do so we utilized Piezo-specific RNAi in combination with different sensor fly strains. Combining the GCaMP6medium sensor fly strain with the Piezo RNAi resulted in flies which express the sensor and deplete Piezo in nephrocytes simultaneously. Recording of the Ca^{++} signals did show a significant decrease of the Ca^{++} signal intensity (amplitude) upon shear stress after depletion of Piezo, confirming again its activity in nephrocytes and its involvement in Ca^{++} signalling in these cells **(Figure 5A)**. Quantification of the signal duration (peak duration) and the Ca^{++} (GCAmP6) baseline levels, did not reveal any significant differences between control nephrocytes and cells depleted for Piezo **(Figure 5A)**. Again, we investigated GTPase activity levels in Piezo knockdown nephrocytes, as Ca^{++} signalling was significantly impaired and Ca^{++} is known to be involved in GTPase activation. Interestingly, loss of Piezo did not result in changes of active Rho1 and Rac/Cdc42 levels **(Figure 5B,C)**.

Our data shows that loss of Piezo only results in a mild filtration phenotype, but does not impact on GTPase activation.

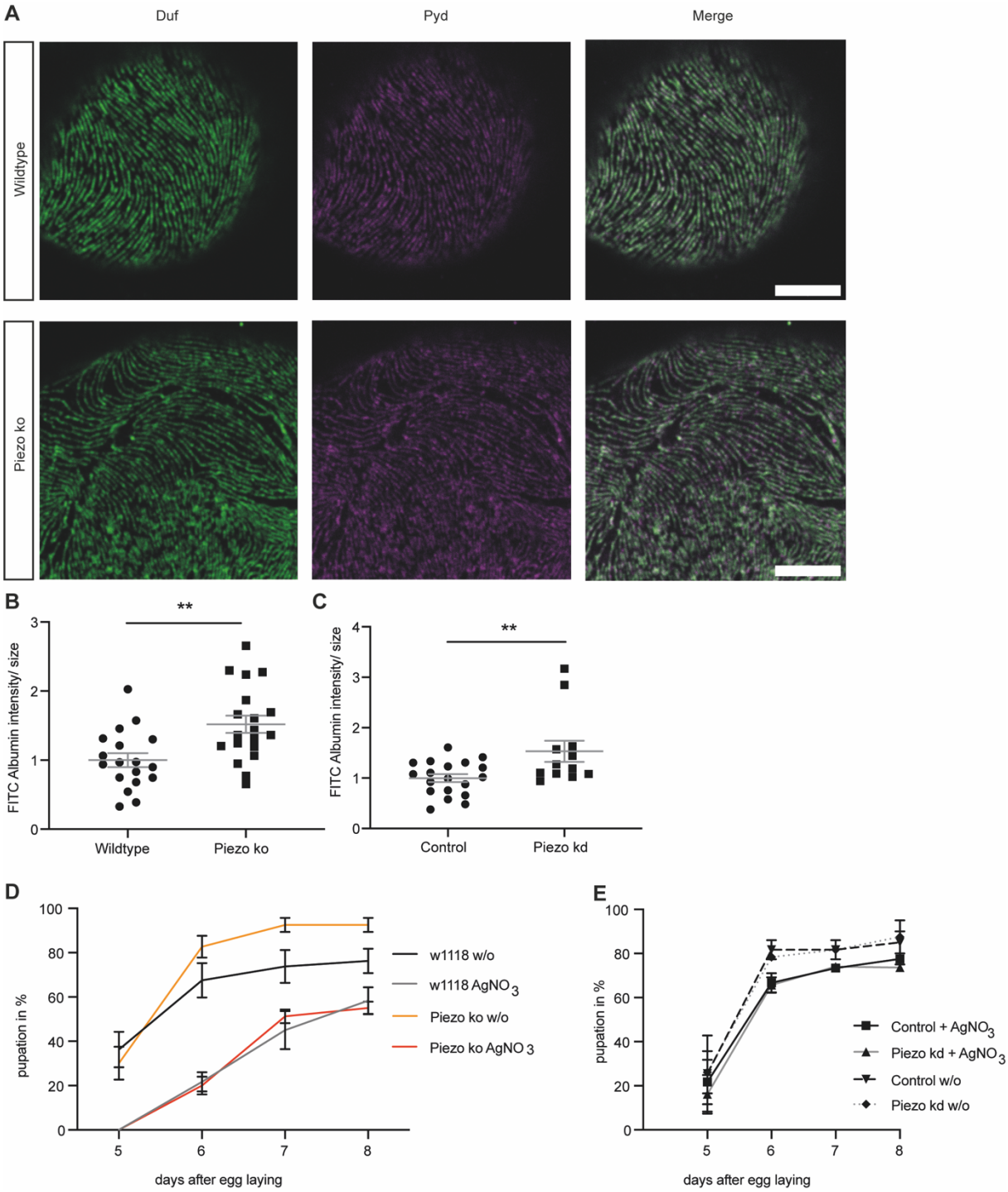

Figure 4: Loss of Piezo caused a mild filtration phenotype. A Immunofluorescence staining with a Duf and Pyd antibody did not reveal any morphological changes in Piezo^{ko} (w;+;*piezo*^{ko}) nephrocytes in comparison to control cells (wildtype w^{1118}). Scale bar 5 = µm. **B,C** FITC Albumin uptake assays revealed a filtration defect with an increased FITC-Albumin uptake in Piezo^{ko} and Piezo knockdown nephrocytes. Student's t-test: **: $p < 0.01$. Control: w;*sns*-Gal4/+;UAS-*dicer2*/+; Piezo kd: w;*sns*-Gal4/ UAS-*piezo*-RNAi;UAS-*dicer2*/+. **D** $AgNO_3$ toxin assays did not revealed a filtration defect, as Piezo^{ko} flies showed a similar delay in pupation when compared to controls (wildtype w1118). **E** AgNO3 toxin assay using Piezo RNAi also did not reveal any differences in pupation behaviour, when compared to control flies.

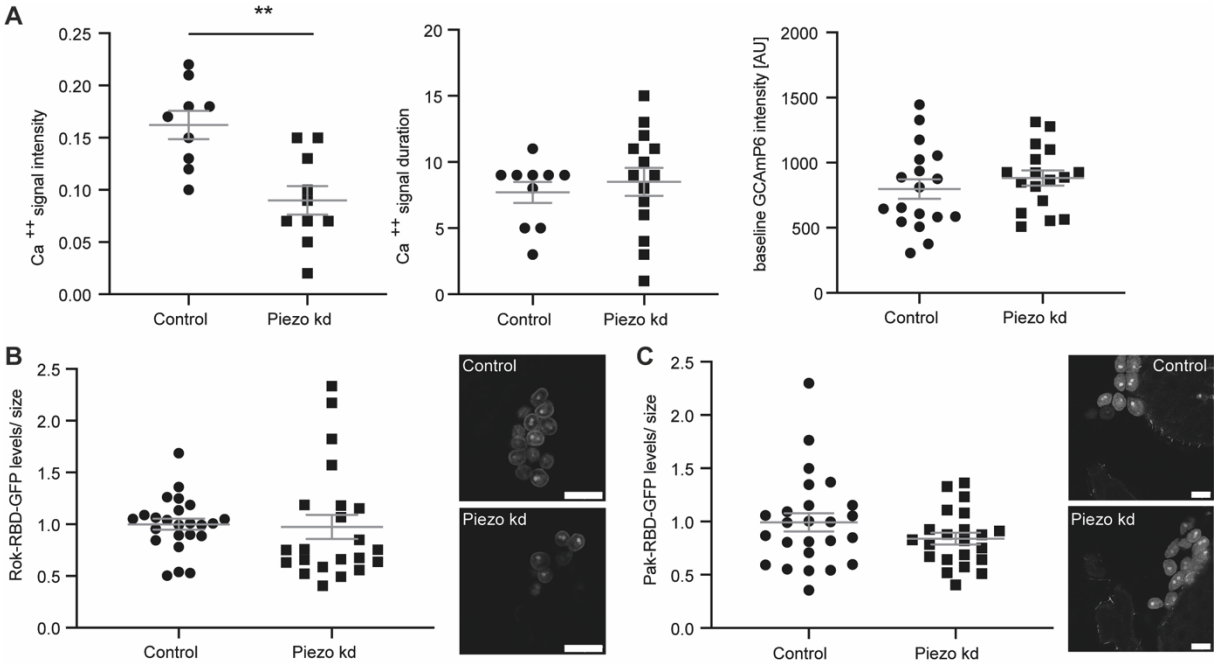

Figure 5: Piezo knockdown resulted in impaired Ca^{++} signalling, but did not affect GTPase activation. A Ca^{++} imaging and quantification of the GCAmP6 signal did reveal a significant decrease in signal intensity after depletion of Piezo. Signal duration and baseline Ca^{++} (GCAmP6) levels were not changed upon loss of Piezo. Control: w; *sns*-Gal4/+;UAS-*GCAmP6m*/+; Piezo kd: w; *sns*-Gal4/UAS-*piezo*-RNAi;UAS-*GCAmP6m*/+. Student's t-test: **: $p < 0.01$. **B** Quantification of the Rho1 (Rok-RBD-GFP) and **C** Rac/Cdc42 (Pak-RBD-GFP) activity levels in Piezo depleted cells did not reveal any differences to control cells. (scale bar = 50μm (**B**) = 25μm(**C**)). Control: w; *sns*-Gal4/+;UAS-*rok-RBD-GFP*/+; Piezo kd: w; *sns*-Gal4/UAS-*piezo*-RNAi;UAS-*rok-RBD-GFP*/+ (**B**); Control: w; *sns*-Gal4/+;sqh-*pak-RBD-GFP*/+; Piezo kd: w; *sns*-Gal4/UAS-*piezo*-RNAi;sqh-*pak-RBD-GFP*/+ (**C**).

Elevated Piezo levels caused a severe filtration phenotype, significantly increased Rho1-GTP levels and actin stress fibre formation

Piezo activation with YODA confirmed the presence of Piezo in nephrocytes and its involvement in a mechanotransduction pathway including Ca^{++} signalling and GTPases. Depletion of Piezo by knockout and knockdown revealed a mild filtration defect, but no impact on GTPase activation. As pharmacological activation of Piezo resulted in increased active Rho1 levels, which are described to be detrimental for podocyte biology [37], and loss of Piezo only caused a mild phenotype, we further investigated whether an overexpression of the channel results in a severe nephrocyte phenotype. In contrast to the acute intervention by YODA application, overexpression

of Piezo in nephrocytes is a chronic intervention, which gives the cells days to manifest a phenotype.

First, we studied the effect on Ca^{++} signalling. We induced shear stress after 60 secs by pipetting buffer on the tissue (red arrow) and observed an immediate Ca^{++} peak in controls **(Figure 6A)**. Imaging Piezo overexpression cells revealed a constant oscillating Ca^{++} signal and no additional peak when applying shear stress (red arrow) **(Figure 6B)**. These constant, force-independent oscillations are consistent with elevated levels of a Ca^{++} permeable channel, due to overexpression of Piezo. Whether the increased number of channels at the nephrocyte diaphragm also causes an opening of the channels, remains unclear. **(Figure 6A,B)**.

We then analysed the impact of increased Piezo levels on nephrocyte morphology and function. The UAS-Gal4 system we are using to express Piezo in nephrocytes can be modulated by temperature, which enables us to increase expression levels with temperature. We used two different temperatures (medium: 25°C and high: 28°C) for Piezo overexpression. Of note, all other experiments (pharmacological activation and Piezo depletion) were performed at 25°C.

Our data show, that morphology was not impacted by Piezo overexpression at 28°C (high levels) **(Figure 6C).** FITC Albumin uptake was significantly increased in cells expressing high levels (28°C) when compared to control cells **(Figure 6D)**. Interestingly, the $AgNO_3$ toxin assay revealed a severe filtration defect already at 25°C, with a significant delay of pupation detectable from day 5 **(Figure 6E)**.

Next, we investigated the impact of increased Piezo levels on GTPase activation. Overexpression of Piezo resulted in significantly increased Rho1-GTP levels, while active Rac/Cdc42 levels were not altered **(Figure 6F,G)**. We observed the same effect for active Rho1 levels, when treating cells with YODA. As activation of Rho1 was described to cause actin stress fibre formation in podocytes [41], we again visualized the

actin cytoskeleton with LifeAct-RFP. A previous study investigated the actin cytoskeleton in nephrocytes and could show the presence of cortical stress fibres and actin clusters in the cells [40]. Interestingly and in line with the activation of Rho1, overexpression of Piezo caused a significant increase of both, cortical actin fibres and actin clusters, when compared to controls **(Figure 6H)**. This finding is in contrast to the acute Piezo activation by YODA application and suggests a more severe phenotype when Piezo levels are permanently increased and active (chronic effect). Our data again confirms that Piezo is involved in regulating Ca^{++} signalling and Rho1 activation and also shows that changes of the actin cytoskeleton are part of the adaptive behaviour in response to the mechanotransduction pathway as well.

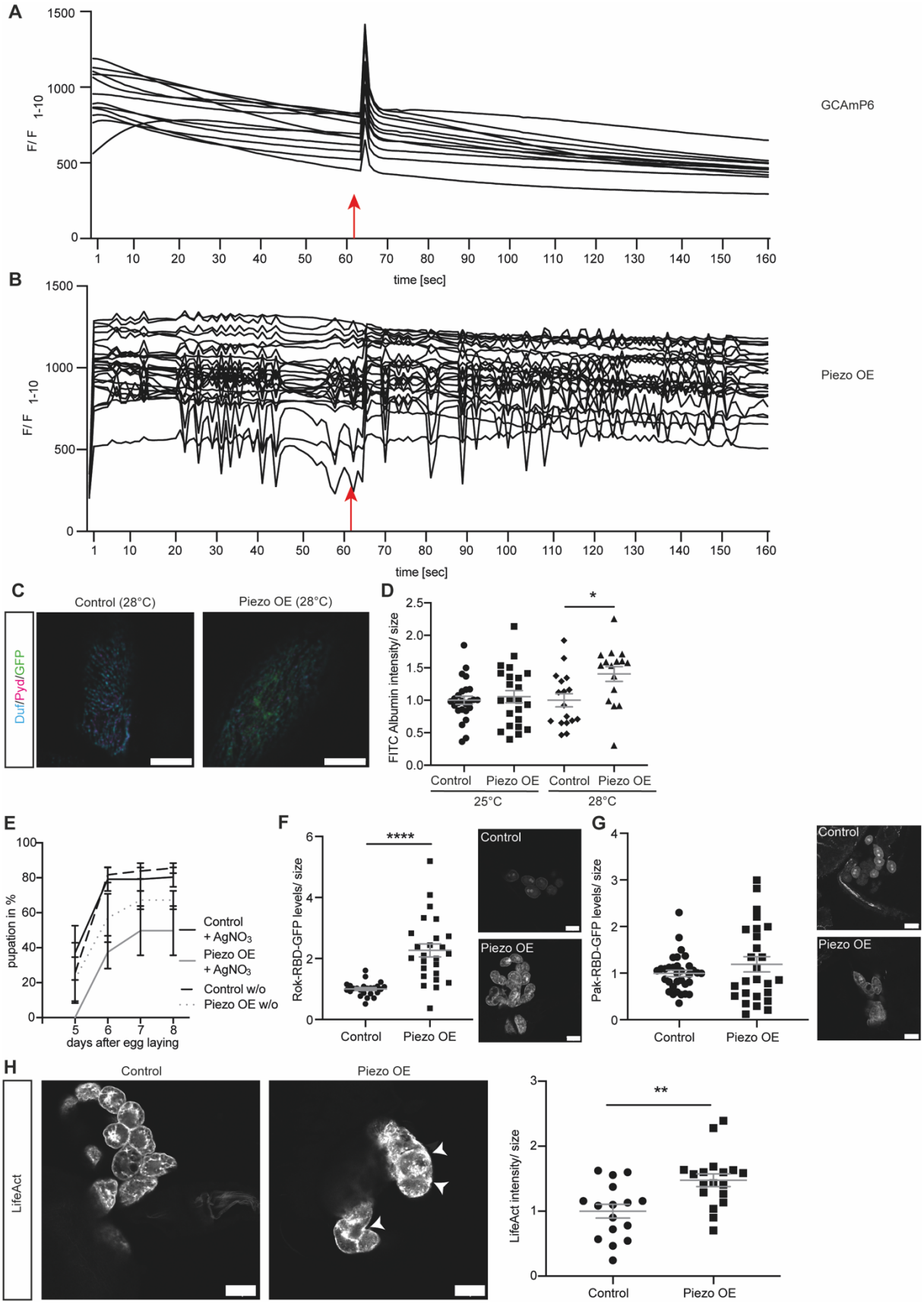

Figure 6: Elevated Piezo levels cause a severe filtration phenotype and result in elevated Rho1-GTP levels and more actin stress fibers. A Ca^{++} imaging of GCAmP6 expressing nephrocytes revealed an immediate increase of the GCAmP signal/amplitude after inducing shear stress by adding buffer (red arrow). Depicted is one animal and one curve is one nephrocyte. Images were taken every

second for 150secs. For analysis and quantification values were normalized to F_{1-10}. Control: w; *sns*-Gal4/+;UAS-*GCAmP6m*/+. **B** Ca^{++} imaging of nephrocytes expressing Piezo and GCAmP6 simultaneously. The elevated Piezo levels resulted in a constant oscillating GCAmP6 intensity pattern. Inducing shear stress by adding buffer did not result in an immediate increase of the intensity as observed for controls. Depicted is one animal and one curve is one nephrocyte. Images were taken every second for 150secs. For analysis and quantification values were normalized to F_{1-10}. Piezo OE: w; *sns*-Gal4/+;UAS-*GCAmP6m*/UAS-*piezo*-GFP. **C** Immunofluorescence staining with a Duf (cyan) and Pyd (magenta) antibody did not reveal any morphological changes in nephrocytes expressing Piezo (green). Flies were kept at 28°C to increase protein expression levels. Scale bar = 25μm. Control: w; *sns*-Gal4/+;UAS-*dicer2*/+. Piezo OE: w; *sns*-Gal4/+;UAS-*dicer2*/UAS-*piezo*-GFP. **D** FITC Albumin assays revealed a significantly increased FITC Albumin uptake in nephrocytes expressing Piezo at 28°C, while no filtration defect was observed at 25°C. Student's t-test: *: $p < 0.05$. **E** AgNO3 toxin assays confirmed a severe filtration defect, as larvae expressing Piezo in nephrocytes present with a significantly delayed pupation behaviour already at 25°C. 2way-ANOVA with Tukey's multiple comparison test: *: $p < 0.05$. **F** Piezo expression caused a significant increase of active Rho1 levels in nephrocytes. Student's t-test: ****: $p < 0.0001$. Scale bar = 25μm. Control: w; *sns*-Gal4/+;UAS-*rok-RBD*-GFP/+. Piezo OE: w; *sns*-Gal4/+;UAS-*rok-RBD*-GFP/UAS-*piezo*-GFP. **G** Rac-GTP levels were not altered upon expression of Piezo in nephrocytes. Scale bar = 25μm. Control: w; *sns*-Gal4/+;sqh-*pak-RBD*-GFP/+. Piezo OE: w; *sns*-Gal4/+;sqh-*pak-RBD*-GFP/UAS-*piezo*-GFP. **H** Visualisation of the actin cytoskeleton revealed an increase of cortical actin stress fibers (arrow heads) and actin clusters in nephrocytes expressing Piezo. Quantification was done for the whole cell. Student's t-test: **: $p < 0.01$. Scale bar = 25μm. Control: w; *sns*-Gal4/+;UAS-*LifeACT*-RFP/+. Piezo OE: w; *sns*-Gal4/+;UAS-*LifeACT*-RFP/UAS-*piezo*-GFP.

Pharmacological inhibition with tarantula toxin reversed the elevated Rho1-GTP levels in Piezo overexpressing cells

Overexpression of Piezo resulted in a severe nephrocyte phenotype including filtration disturbances, significantly increased Rho1-GTP levels and more actin stress fibres and clusters. Therefore, we tested whether pharmacological inhibition of the channel could reverse the phenotype and be beneficial for nephrocyte function. To do so, we used tarantula toxin (GSMTx4), which integrates into the cell membrane and blocks the opening of the channel upon mechanical stretch [42] .

Acute inhibition of the mechanosensitive channel did not result in a morphology or filtration function phenotype **(Figure 7A,B)**. GTPases assessment and analysis of the actin cytoskeleton also did not reveal significant differences in comparison to control cells **(Figure 7C,D,E,F)**. Overexpression of Piezo caused a highly significant increase of active Rho1 levels, hence we treated the Piezo overexpression nephrocytes with tarantula toxin and quantified Rho1-GTP levels. 5 min treatment with

the toxin significantly reduced the Rho1-GTP levels and resulted in a rescue **(Figure 7G).** Taken together, our data demonstrates that tarantula toxin can be used to reverse the overactive Piezo effect on GTPase activation. A treatment with the toxin did not reveal any pathological effects on nephrocyte morphology and function and can therefore be used as an intervention.

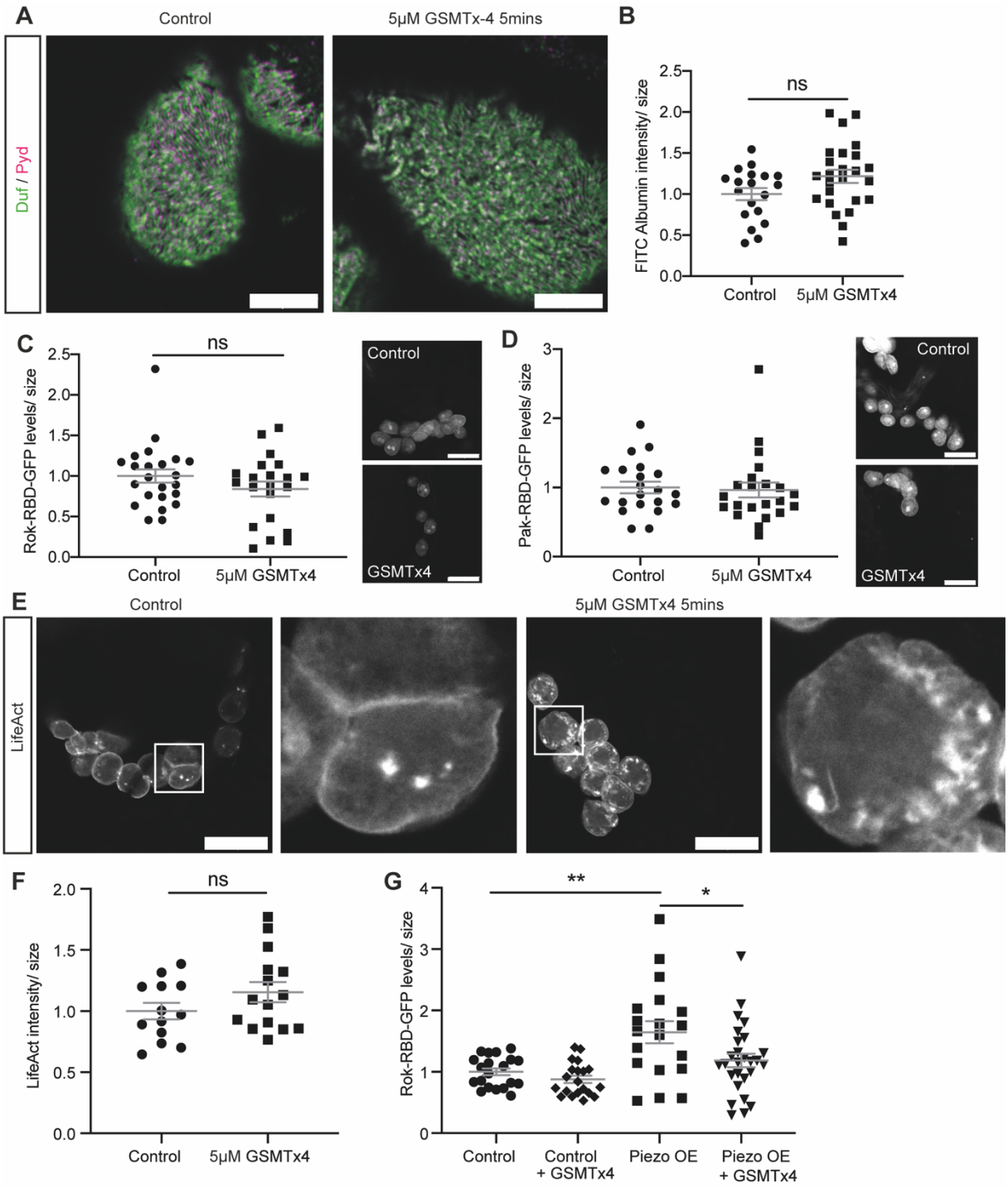

Figure 7: GSMTx4 treatment did not result in a nephrocyte phenotype and reversed elevated Rho1 activity levels in Piezo overexpression cells. A Immunofluorescence staining with Duf and Pyd antibodies did not reveal any morphological changes after incubation with 5μM GSMTx4 for 5 min. Scale bar = 5 μm. **B** FITC Albumin uptake assays did not reveal any differences between controls and nephrocytes incubated with GSMTx4 for 5 min. **C,D** Quantification of GTPase activity levels did not reveal any changes in Rho1-GTP (Rok-RBD-GFP) or Rac/Cdc42-GTP (Pak-RBD-GFP) levels. Scale bar = 50 μm. Rok-GFP: w; *sns*-Gal4/+;UAS-*dicer2*/UAS-*rok*-*RBD*-GFP (**C**). Pak-GFP: w; *sns*-Gal4/+;UAS-*dicer2*/sqh-*pak*-*RBD*-GFP (**D**). **E,F** Visualization of the actin cytoskeleton did not show a significant increase of actin clusters after incubation of nephrocytes with GSMTx4 for 5 min. Scale bar = 50 μm. w; *sns*-Gal4/+;UAS-*dicer2*/UAS-*LifeACT*-RFP. **G** Rho1 activity levels were significantly reduced in Piezo overexpressing cells (w; *sns*-Gal4/+; UAS-*rok*-*RBD*-GFP/UAS-*Piezo*-GFP) after 5 min treatment with GSMTx4. Comparison with control cells revealed a very good rescue, as Rho1-GTP levels were not significantly higher in Piezo overexpressing cells treated with GSMTx4 when compared to controls (w; *sns*-Gal4/+; UAS-*rok*-*RBD*-GFP/+). 1-Way ANOVA with Tukey's multiple comparison test: *: $p < 0.05$; **: $p < 0.01$.

Piezo1 and Piezo2 levels are altered upon glomerular disease

To unravel whether Piezo also plays a role in glomerular disease, we analysed gene array data from the European Renal cDNA Bank (ERCB, UKE Hamburg). Piezo1 levels are decreased in glomerular patient derived tissue from membranous glomerulonephritis (MGN) and systemic lupus erythematosus nephritis (SLE) **(Figure 8A)**, while Piezo2 levels were upregulated in all disease entities tested, among them FSGS (Focal segmental glomerulosclerosis), membranous glomerulonephritis (MGN) and systemic lupus erythematosus nephritis (SLE) **(Figure 8A)**. Interestingly, Piezo2 levels are also increased in glomerular tissue obtained from patients suffering from hypertension (HT) **(Figure 8A)**. To further investigate, whether the alterations in Piezo1 and Piezo2 levels are elicited by expression changes in podocytes, we performed immunofluorescence staining in kidney tissue obtained from patients (Institute of Pathology, UKE Hamburg) **(Figure 8B, Supp. Figure 1)**. We observed some podocytes with an increased expression of Piezo2, however this increase seems to be rather mild. In addition, we observed a re-localisation of Piezo2 upon injury. Piezo2 localizes close to areas where Synaptopodin is expressed (arrowheads with notch) in heathy controls, but the localisation pattern of the two proteins is still distinct.

However, we observed clear co-localisation (arrowheads) of both proteins in the different injury types **(Figure 8B, Supp. Figure 1)**. Whether this co-localisation happens as a result of injury is not known. Also, whether in addition to a slight increase of total protein expression, channel activity is elevated upon podocyte injury remains unknown.

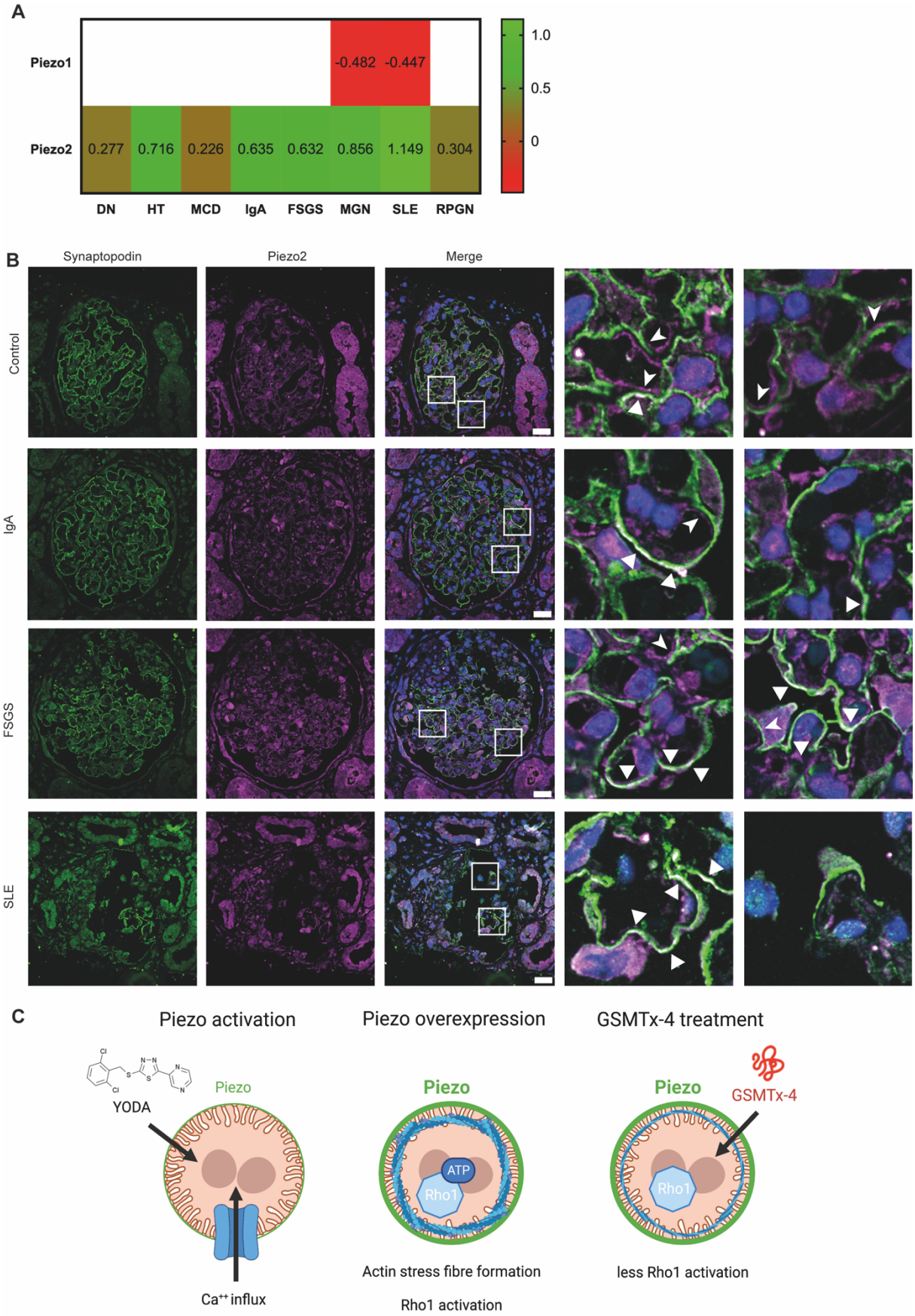

Figure 8: Piezo 1 and Piezo 2 levels are altered upon glomerular disease. A Analysing gene expression profiles from patients with different disease entities from the ERCB data base revealed a down-regulation of Piezo 1 in membranous glomerulonephritis (MGN) and systemic lupus erythematosus nephritis (SLE), while Piezo 2 was upregulated in all disease entities tested. DN: Diabetic

nephropathy; HT: Hypertension; MCD: Minimal Change Disease; IgA: IgA nephropathy; FSGS: Focal segmental glomerulosclerosis; RPGN: Rapidly progressive glomerulosclerosis. **B** Immunofluoresence staining visualizes Piezo 2 and Synaptopodin in control and injury tissue. While only slight increase of Piezo 2 expression levels were observed upon injury in podocytes, Piezo 2 re-localizes to areas where Synaptopodin is expressed upon injury. (arrowheads with notch: separated Piezo 2 and Synaptopodin expression; arrowheads: co-localisation of Piezo 2 and Synaptopodin) Scale bar = 25μm. **C** Piezo localizes to the nephrocyte diaphragm and co-localizes with Duf and Pyd. Activation of the channel with its agonist YODA results in an increased Ca^{++} signal and activation of Rho1 (left panel). Elevated Piezo levels have a pathological effect on nephrocyte biology and cause a severe filtration defect. In line with the YODA effects, elevated Piezo levels also result in activation of Rho1 and an increased formation of cortical actin stress fibers and actin clusters (middle panel). Treatment with the antagonist GSMTx4, tarantula toxin, can reverse the elevated Rho1-GTP levels upon increased Piezo levels, exhibiting a potential as a future therapeutic (right panel). Images created with BioRender.com.

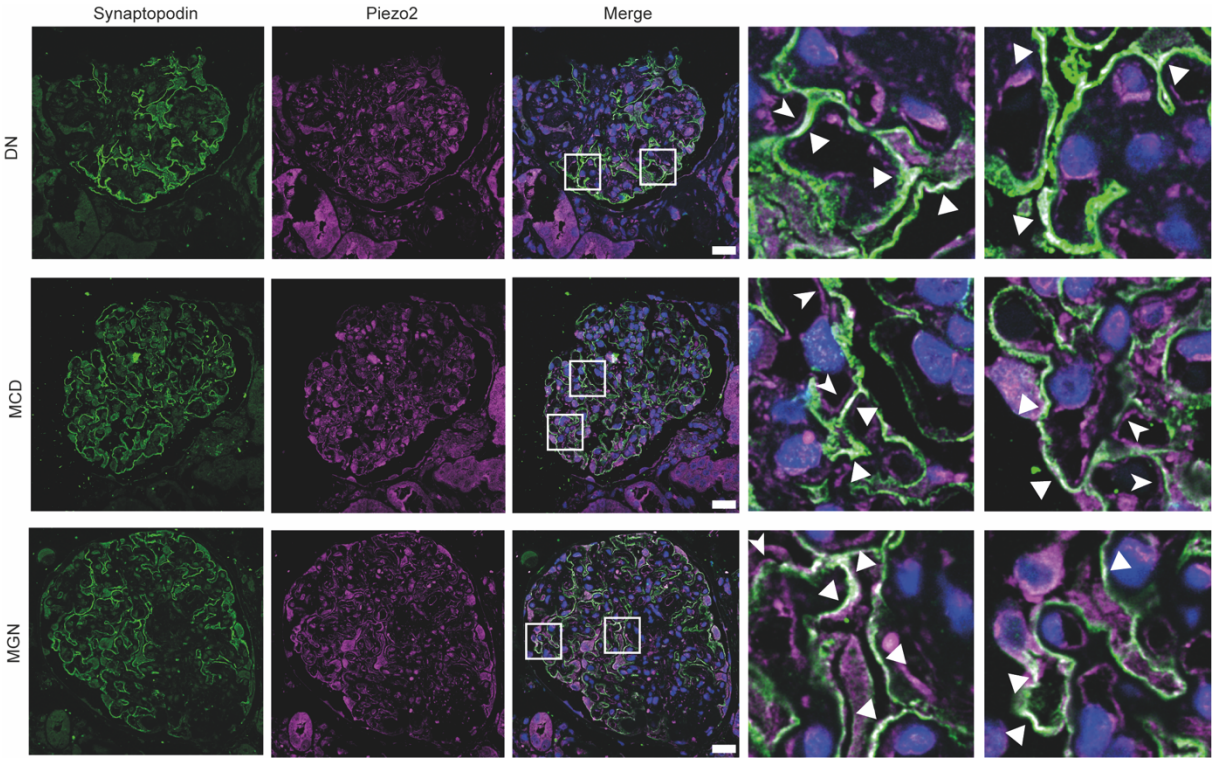

Supp. Figure 1: Expression of Piezo 2 in glomerular injury. Immunostaining visualizing Piezo 2 and Synaptopodin in patient derived tissue revealed a slight increase of Piezo 2 levels in podocytes and a re-localisation to areas in which Synaptopodin is expressed. DN: Diabetic nephropathy, MCD: Minimal Change Disease, MGN: membranous glomerulonephritis, RPGN: Rapidly progressive glomerulosclerosis. (arrowheads with notch: separated Piezo 2 and Synaptopodin expression; arrowheads: co-localisation of Piezo 2 and Synaptopodin) Scale bar = 25μm.

Discussion

Mechanotransducers play a crucial role in podocyte biology and within this study, we were able to delineate the physiological role of the mechano-sensitive ion channel Piezo in nephrocytes for the first time. Here, we provide evidence that Piezo is expressed at the nephrocyte diaphragm and co-localizes with Duf, the NEPH

homolog in the fly, suggesting Piezo to be a novel component of the diaphragm protein complex. Our data shows that Piezo is involved in a mechanotransduction pathway, which includes Ca^{++} signalling, Rho1 activation and subsequently actin stress fibre and actin cluster formation in nephrocytes. Moreover, an increase of protein levels results in filtration disturbances in nephrocytes **(Figure 8C)**.

We also confirmed that nephrocytes respond to shear stress by opening mechanosensitive channels resulting in Ca^{++} influx. This response is significantly reduced upon injury by depleting Duf (dNEPH) or Sns (dNephrin). Loss of either of those nephrocyte diaphragm proteins results in a severe morphological phenotype, with loss of the lacunae structure and degradation of the nephrocyte diaphragm [26,27]. Whether mechanosensitive channels are degraded as well or misslocalized remains an open question. In a recent study, Sivakumar et al. showed that nephrocytes exhibit stochastic Ca^{++} waves *in vivo* [43]. They were able to show a functional role of store operated Ca^{++} entry (SOCE) mechanisms, in particular Stim and Orai-dependent, on nephrocyte endocytosis [43]. These findings confirm our hypothesis of Ca^{++} signalling as an important signalling feature in *Drosophila* nephrocytes.

The tight regulation of GTPases is essential to maintain podocyte health and survival. Previous studies revealed a pathological effect of overactive RhoA and Rac1 in mice. This includes albuminuria as well as foot process effacement and the activation of both is associated with FSGS and minimal change disease [37–39]. In line with this, the overactivation of Rho1 in nephrocytes also resulted in a severe nephrocyte phenotype with morphological and functional disturbances [44]. Mechanosensors, such as TRP channels, also have been described to regulate GTPase activation in podocytes [45]. One downstream target of GTPases is the actin cytoskeleton, which plays an essential role during podocyte injury and rearrangement processes [46]. Here, we identified increased activation of Rho1 after YODA treatment

and overexpression of Piezo. In addition, YODA treatment caused decreased Rac1 activity levels but did not change the actin cytoskeleton. One potential explanation is that acute activation of Piezo might not affect the actin cytoskeleton. Also, the short time between YODA incubation and imaging the cells, might not be sufficient to observe actin stress fibre formation. The impact of over-active Rho1 on the actin cytoskeleton in nephrocytes remains unknown, but the expression of an constitutively active Rho1 variant resulted in a severe nephrocyte phenotype, including morphological changes and filtration disturbances [44]. In cultured podocytes, the expression of over-active RhoA (Rho1 in *Drosophila*) caused a significant increase of actin stress fibres [41], a similar effect to what we observed in the Piezo overexpression nephrocytes.

Our findings, that GTPase activation and subsequent actin stress fibre formation are crucial aspects of the podocytes response to injury, are supported by a previous study investigating the effect of Bis-T-23 in podocytes. Bis-T-23 promotes actin-dependent dynamin oligomerization and stabilizes the actin cytoskeleton during podocyte injury [47]. In detail, several injury models which caused actin-cytoskeleton rearrangement could be at least partially rescued by Bis-T-23 treatment, again emphasising the importance of the actin-cytoskeleton and upstream regulators such as GTPases [47].

Due to their position podocytes are constantly facing changing biomechanical forces such as hydrostatic pressure and shear stress. Therefore, it is not surprising that recent studies identified mechanosensors to play a crucial role for podocyte biology. Among them are Talin [17], Vinculin [48] and Filamin [8,9,18]. The mechano-sensitive ion channel Piezo1 has recently been found to be expressed in mouse podocytes, but its exact localisation pattern and its functional role in these cells is not known [19]. Within our study, we were able to show that Piezo1 and Piezo2 are expressed ubiquitously in mouse podocytes. In human tissue, Piezo2 also exhibits a linear localisation pattern,

which is close to areas where Synaptopodin is expressed, but localisation of both proteins is still distinct. Interestingly, glomerular Piezo2 levels are increased upon injury and Piezo2 seems to re-localizes to areas in which Synaptopodin is expressed upon injury in podocytes. Whether this re-localisation is a result of the injury remains unknown. Also, whether activity of Piezo2 is increased during podocyte injury is not known.

Overactive variants might result in pathological effects and glomerular disease phenotypes. A recent publication identified a gain-of-function mutation present in a third of the African population, which results in the resistance to plasmodium infection due to dehydrated red blood cells [49]. Clinical evaluation of individuals carrying this allele will be of greatest interest, in particular in regard to kidney function.

Assuming a correlation between over-active Piezo variants and a glomerular disease phenotype a treatment to block Piezo activation could be beneficial for patients. Our data showed that the treatment with tarantula toxin (GSMTx4) was able to reverse the increased Rho1-GTP levels. Interestingly, GSMTx4 is currently used in clinical trials as a novel treatment for muscle dystrophy (https://laforcedmd.com/tarantula-venom-dmd/) and would therefore be an ideal candidate for patients suffering from Piezo over-activation induced glomerular disease. Of note, GSMTx4 is not a specific Piezo inhibitor and can affect other mechano-sensitive channels as well. Also, systemic effects of GSMTx4 application cannot be ruled out at the moment. Nonetheless, GSMTx4 seems to be a promising novel therapeutic.

Taken together, here we provide evidence that the mechano-sensitive ion channel Piezo is localizing to the nephrocyte and slit diaphragm, needs to be tightly controlled to maintain nephrocyte morphology and function and regulates Rho1 activity levels and the formation of actin stress fibres via Ca^{++} influx.

Author contribution

S.K. conceived the study, analysed the data, made the figures and drafted the paper, S.K., I.E. and M.L. performed experiments, T.W. provided patient material, B.D. and T.B.H. revised the study critically for important intellectual content, S.K. and B.D. revised the paper; all authors approved the final version of the manuscript.

Acknowledgement

The Anti-Pyd monoclonal antibody developed by Fanning [50] was obtained from the Developmental Studies Hybridoma Bank, created by the NICHD of the NIH and maintained at The University of Iowa, Department of Biology, Iowa City, IA 52242. We also thank all participating centres of the European Renal cDNA Bank - Kröner-Fresenius biopsy bank (ERCB-KFB) and their patients for their cooperation. Images were created with BioRender.com.

Funding

S.K. received funding from the German Research Foundation (KO 6045/1-1). T.W. received funding from the German Research Foundation (CRC1192). T.B.H. received funding from the German Research Foundation (CRC1192, HU 1016/8-2, HU 1016/11-1, HU 1016/ 12-1). S.K. and T.B.H received funding from the BMBF (STOP-FSGS-01GM1901C).

Conflict of Interest

None. The authors have nothing to disclose.

Literatur

1. Pavenstädt, H., Kriz, W. & Kretzler, M. Cell biology of the glomerular podocyte. *Physiol. Rev.* **83**, 253–307 (2003).
2. Kestilä, M. *et al.* Positionally cloned gene for a novel glomerular protein--

nephrin--is mutated in congenital nephrotic syndrome. *Mol. Cell* **1**, 575–582 (1998).
3. Boute, N. *et al.* NPHS2, encoding the glomerular protein podocin, is mutated in autosomal recessive steroid-resistant nephrotic syndrome. *Nat. Genet.* **24**, 349–354 (2000).
4. Kaplan, J. M. *et al.* Mutations in ACTN4, encoding alpha-actinin-4, cause familial focal segmental glomerulosclerosis. *Nat. Genet.* **24**, 251–256 (2000).
5. Winn, M. P. *et al.* A mutation in the TRPC6 cation channel causes familial focal segmental glomerulosclerosis. *Science* **308**, 1801–1804 (2005).
6. Hildebrandt, F. Genetic kidney diseases. *Lancet Lond. Engl.* **375**, 1287–1295 (2010).
7. Markowitz, G. S., Bomback, A. S. & Perazella, M. A. Drug-Induced Glomerular Disease: Direct Cellular Injury. *Clin. J. Am. Soc. Nephrol.* **10**, 1291–1299 (2015).
8. Koehler, S. *et al.* Proteome Analysis of Isolated Podocytes Reveals Stress Responses in Glomerular Sclerosis. *J. Am. Soc. Nephrol. JASN* **31**, 544–559 (2020).
9. Greiten, J. K. *et al.* The role of filamins in mechanically stressed podocytes. *FASEB J. Off. Publ. Fed. Am. Soc. Exp. Biol.* **35**, e21560 (2021).
10. Feng, D., DuMontier, C. & Pollak, M. R. Mechanical challenges and cytoskeletal impairments in focal segmental glomerulosclerosis. *Am. J. Physiol. -Ren. Physiol.* **314**, F921–F925 (2018).
11. Endlich, N. *et al.* Podocytes respond to mechanical stress in vitro. *J. Am. Soc. Nephrol. JASN* **12**, 413–422 (2001).
12. Endlich, K., Kliewe, F. & Endlich, N. Stressed podocytes-mechanical forces, sensors, signaling and response. *Pflugers Arch.* **469**, 937–949 (2017).
13. Kriz, W. & Lemley, K. V. Mechanical challenges to the glomerular filtration barrier: adaptations and pathway to sclerosis. *Pediatr. Nephrol.* **32**, 405–417 (2017).
14. Kriz, W. & Lemley, K. V. A Potential Role for Mechanical Forces in the Detachment of Podocytes and the Progression of CKD. *J. Am. Soc. Nephrol.* **26**, 258–269 (2015).
15. Wiggins, J. E. *et al.* Podocyte hypertrophy, 'adaptation,' and 'decompensation' associated with glomerular enlargement and glomerulosclerosis in the aging rat: prevention by calorie restriction. *J. Am. Soc. Nephrol. JASN* **16**, 2953–2966 (2005).
16. Rinschen, M. M. *et al.* YAP-mediated mechanotransduction determines the podocyte's response to damage. *Sci. Signal.* **10**, (2017).
17. Tian, X. *et al.* Podocyte-associated talin1 is critical for glomerular filtration barrier maintenance. *J. Clin. Invest.* **124**, 1098–1113 (2014).
18. Okabe, M. *et al.* Indirect podocyte injury manifested in a partial podocytectomy mouse model. *Am. J. Physiol. Renal Physiol.* (2021) doi:10.1152/ajprenal.00602.2020.
19. Dalghi, M. G. *et al.* Expression and distribution of PIEZO1 in the mouse urinary tract. *Am. J. Physiol.-Ren. Physiol.* **317**, F303–F321 (2019).
20. Coste, B. *et al.* Piezo1 and Piezo2 are essential components of distinct mechanically activated cation channels. *Science* **330**, 55–60 (2010).
21. Coste, B. *et al.* Piezo proteins are pore-forming subunits of mechanically activated channels. *Nature* **483**, 176–181 (2012).
22. Cahalan, S. M. *et al.* Piezo1 links mechanical forces to red blood cell volume. *eLife* **4**, (2015).
23. Ranade, S. S. *et al.* Piezo1, a mechanically activated ion channel, is required for vascular development in mice. *Proc. Natl. Acad. Sci. U. S. A.* **111**, 10347–10352 (2014).
24. Retailleau, K. *et al.* Piezo1 in Smooth Muscle Cells Is Involved in Hypertension-Dependent Arterial Remodeling. *Cell Rep.* **13**, 1161–1171 (2015).

25. Zhong, M., Komarova, Y., Rehman, J. & Malik, A. B. Mechanosensing Piezo channels in tissue homeostasis including their role in lungs. *Pulm. Circ.* **8**, 2045894018767393 (2018).
26. Weavers, H. *et al.* The insect nephrocyte is a podocyte-like cell with a filtration slit diaphragm. *Nature* **457**, 322–326 (2009).
27. Zhuang, S. *et al.* Sns and Kirre, the Drosophila orthologs of Nephrin and Neph1, direct adhesion, fusion and formation of a slit diaphragm-like structure in insect nephrocytes. *Dev. Camb. Engl.* **136**, 2335–2344 (2009).
28. Hermle, T., Braun, D. A., Helmstädter, M., Huber, T. B. & Hildebrandt, F. Modeling Monogenic Human Nephrotic Syndrome in the Drosophila Garland Cell Nephrocyte. *J. Am. Soc. Nephrol. JASN* **28**, 1521–1533 (2017).
29. Koehler, S. *et al.* Single and Transient Ca(2+) Peaks in Podocytes do not induce Changes in Glomerular Filtration and Perfusion. *Sci. Rep.* **6**, 35400 (2016).
30. Cohen, C. D., Frach, K., Schlöndorff, D. & Kretzler, M. Quantitative gene expression analysis in renal biopsies: a novel protocol for a high-throughput multicenter application. *Kidney Int.* **61**, 133–140 (2002).
31. Cohen, C. D. *et al.* Comparative promoter analysis allows *de novo* identification of specialized cell junction-associated proteins. *Proc. Natl. Acad. Sci.* **103**, 5682–5687 (2006).
32. Tusher, V. G., Tibshirani, R. & Chu, G. Significance analysis of microarrays applied to the ionizing radiation response. *Proc. Natl. Acad. Sci.* **98**, 5116–5121 (2001).
33. Reiser, J. *et al.* TRPC6 is a glomerular slit diaphragm-associated channel required for normal renal function. *Nat. Genet.* **37**, 739–744 (2005).
34. Rinschen, M. M. *et al.* A Multi-layered Quantitative In Vivo Expression Atlas of the Podocyte Unravels Kidney Disease Candidate Genes. *Cell Rep.* **23**, 2495–2508 (2018).
35. Syeda, R. *et al.* Chemical activation of the mechanotransduction channel Piezo1. *eLife* **4**, (2015).
36. Botello-Smith, W. M. *et al.* A mechanism for the activation of the mechanosensitive Piezo1 channel by the small molecule Yoda1. *Nat. Commun.* **10**, 4503 (2019).
37. Zhu, L., Jiang, R., Aoudjit, L., Jones, N. & Takano, T. Activation of RhoA in podocytes induces focal segmental glomerulosclerosis. *J. Am. Soc. Nephrol. JASN* **22**, 1621–1630 (2011).
38. Yu, H. *et al.* Rac1 activation in podocytes induces rapid foot process effacement and proteinuria. *Mol. Cell. Biol.* **33**, 4755–4764 (2013).
39. Robins, R. *et al.* Rac1 activation in podocytes induces the spectrum of nephrotic syndrome. *Kidney Int.* **92**, 349–364 (2017).
40. Muraleedharan, S., Sam, A., Skaer, H. & Inamdar, M. S. Networks that link cytoskeletal regulators and diaphragm proteins underpin filtration function in Drosophila nephrocytes. *Exp. Cell Res.* **364**, 234–242 (2018).
41. Wang, L. *et al.* Mechanisms of the proteinuria induced by Rho GTPases. *Kidney Int.* **81**, 1075–1085 (2012).
42. Suchyna, T. M. *et al.* Identification of a peptide toxin from Grammostola spatulata spider venom that blocks cation-selective stretch-activated channels. *J. Gen. Physiol.* **115**, 583–598 (2000).
43. Sivakumar, S., Miellet, S., Clarke, C. & Hartley, P. S. Insect nephrocyte function is regulated by a store operated calcium entry mechanism controlling endocytosis and Amnionless turnover. *J. Insect Physiol.* **143**, 104453 (2022).
44. Koehler, S. *et al.* Par3A and Par3B orchestrate podocyte architecture by

regulating RhoA levels. *bioRxiv* 2020.02.10.933671 (2020) doi:10.1101/2020.02.10.933671.
45. Tian, D. *et al.* Antagonistic regulation of actin dynamics and cell motility by TRPC5 and TRPC6 channels. *Sci. Signal.* **3**, ra77 (2010).
46. Wang, Q. *et al.* Role of Transient Receptor Potential Canonical Channel 6 (TRPC6) in Diabetic Kidney Disease by Regulating Podocyte Actin Cytoskeleton Rearrangement. *J. Diabetes Res.* **2020**, (2020).
47. Schiffer, M. *et al.* Pharmacological targeting of actin-dependent dynamin oligomerization ameliorates chronic kidney disease in diverse animal models. *Nat. Med.* **21**, 601–609 (2015).
48. Lausecker, F. *et al.* Vinculin is required to maintain glomerular barrier integrity. *Kidney Int.* **93**, 643–655 (2018).
49. Ma, S. *et al.* Common PIEZO1 Allele in African Populations Causes RBC Dehydration and Attenuates Plasmodium Infection. *Cell* **173**, 443-455.e12 (2018).
50. Choi, W. *et al.* The single Drosophila ZO-1 protein Polychaetoid regulates embryonic morphogenesis in coordination with Canoe/afadin and Enabled. *Mol. Biol. Cell* **22**, 2010–2030 (2011).